Extraction of Cardiac and Respiratory Motion Information from Cardiac X-Ray Fluoroscopy Images Using Hierarchical Manifold Learning

Maria Panayiotou[1], Andrew P. King[1], Kanwal K. Bhatia[3], R. James Housden[1], YingLiang Ma[1], C. Aldo Rinaldi[1,2], Jas Gill[1,2], Michael Cooklin[1,2], Mark O'Neill[1,2], and Kawal S. Rhode[1]

[1] Division of Imaging Sciences and Biomedical Engineering, King's College London, UK
[2] Department of Cardiology, Guy's & St. Thomas' Hospitals NHS Foundation Trust, London, UK
[3] Biomedical Image Analysis Group, Department of Computing, Imperial College London, London, UK
maria.panayiotou@kcl.ac.uk

Abstract. We present a novel and clinically useful method to automatically determine the regions that carry cardiac and respiratory motion information directly from standard mono-plane X-ray fluoroscopy images. We demonstrate the application of our method for the purposes of retrospective cardiac and respiratory gating of X-ray images. Validation is performed on five mono-plane imaging sequences comprising a total of 284 frames from five patients undergoing radiofrequency ablation for the treatment of atrial fibrillation. We established end-inspiration, end-expiration and systolic gating with success rates of 100%, 100% and 95.3%, respectively. This technique is useful for retrospective gating of X-ray images and, unlike many previously proposed techniques, does not require specific catheters to be visible and works without any knowledge of catheter geometry.

1 Introduction

Electrophysiology (EP) procedures are minimally invasive catheter procedures that are used to treat cardiac arrhythmias. They are carried out under X-ray fluoroscopic image guidance. However, X-ray images have poor soft tissue contrast. To overcome the lack of soft tissue contrast, pre-procedural three-dimensional (3D) images can be registered and overlaid in real-time with the 2D X-ray images using specialized hybrid imaging systems [1]. Achieving the registration in a conventional mono-plane catheter laboratory is challenging. A solution was proposed in [2] where catheters were used to constrain the registration. An implementation of this approach used 3D

O. Camara et al. (Eds.): STACOM 2013, LNCS 8330, pp. 126–134, 2014.

catheter reconstructions from sequential bi-plane X-ray images [3]. This technique required manual cardiac and respiratory phase matching of the bi-plane images. A similar requirement for automatic frame matching exists when catheter positional information needs to be measured with reference to a registered anatomical model. This is important for recording the position of electrical measurements, pacing locations and ablation treatments [4,5].

A cardiac electrocardiogram (ECG) synchronously recorded with X-ray images can be used for cardiac gating. However, this facility is not always present in X-ray systems and when present, there may be unknown delay between the ECG signal and the X-ray data. Respiratory gating can be achieved using breath-holding. This is commonly used during magnetic resonance imaging (MRI) [6]. However, this is impractical in the catheter laboratory where patients can be heavily sedated.

Image-based motion estimation should be more reliable and robust. This approach do not require any special hardware, fiducial markers or additional contrast agent. In [7,8] diaphragm tracking was used for respiratory phase determination. However, the diaphragm is not always visible in cardiac X-ray images due to collimation to reduce radiation dose. A more promising approach is to track the EP catheters [9, 10, 11]. Nevertheless, decoupling the cardiac from the respiratory motion can be challenging. The technique presented in [12] was used to estimate the motion between successive frames using a phase correlation algorithm, without requiring specific catheters to be present. The technique was tested on 2D X-ray angiographic and 3D liver and intra-cardiac ultrasound sequences. The main drawback of this technique is that it assumes that objects in the scene exhibit only translations, which is not the case in EP images.

Manifold learning (ML) has been shown to be a useful image-based method for cardiac and respiratory phase detection. In [13] the Laplacian Eigenmaps (LE) method was used for respiratory gating in MRI and ultrasound (US) applications. In US applications, LE has been used for cardiac gating [14]. In [15] a technique called Hierarchical Manifold Learning (HML) was used to learn the regional correlations in motion within a sequence of time-resolved MR images of the thoracic cavity.

We propose a novel approach for cardiac and respiratory phase gating for cardiac EP X-ray images based on HML. The algorithm is validated using X-ray images taken during radiofrequency ablation (RFA) procedures for patients being treated for atrial fibrillation (AF). The novelty of our approach is that it does not rely on specific catheters being present in the image data or the localisation of these devices, and makes no assumptions about the nature of the motion present in the images.

2 Methods

A block diagram of the proposed method for cardiac and respiratory gating is shown in Fig. 1. We first describe the respiratory gating approach and then outline how this technique is expanded with a number of other image processing operations to make it suitable for cardiac motion gating.

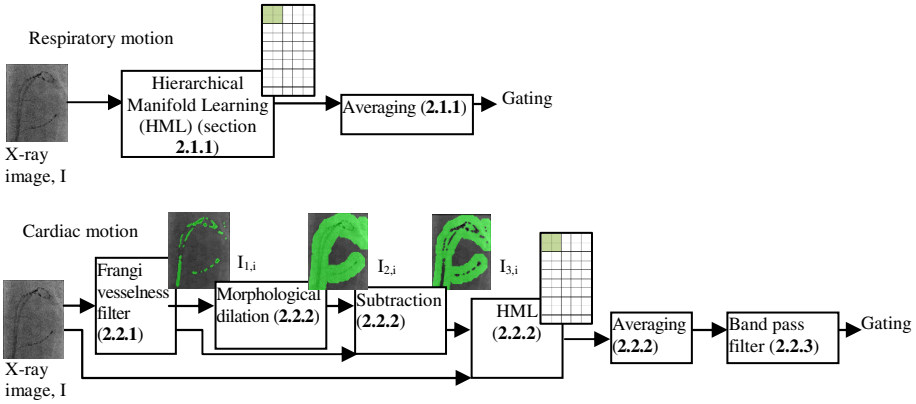

Fig. 1. Block diagram of the proposed HML-based method. (Top) For respiratory gating; (bottom) for cardiac gating.

2.1 Respiratory Gating

2.1.1 Hierarchical Manifold Learning

ML is a non-linear dimensionality reduction technique, which aims to embed data that originally lies in a high dimensional (high-D) space into a lower dimensional (low-D) space, while preserving characteristic properties. LE is a particular ML technique, which is often chosen for medical imaging applications [16]. One of the disadvantages of applying conventional ML techniques to medical images is that the whole of the image is represented by a single value even though not all the image contains relevant information. To prevent this weakness we used HML, a recently proposed technique [15]. To avoid the need to pre-define regions of interest, the images are separated into regular patches, of size 2x2 pixels each, finding a manifold embedding for each image patch. The idea is to align each patch embedding to several parent manifolds, with the strength of the aligning constraint dependent on the distance to parent patch centers. For a 2D image, it would seem natural to constrain a new patch to be close to its four nearest (in terms of distance) parent patches [15]. Consequently, for our experiments, we simply use four (2D) parent patches. As we are trying to recover both the cardiac and respiratory motions, we reduce the data to 2 dimensions. By using a manifold embedding dimensionality of 2, each patch in each time frame is represented by a 2D coordinate. We treated the values in each dimension separately. We found by visual inspection that the coordinates of the 1st dimension represent the respiratory motion while the coordinates of the 2nd dimension represent the cardiac motion. We denote the output of the HML process by P_1, P_2 for the 1st and 2nd dimension, respectively.

2.1.2 Gating

HML is applied to the 2x2 patches of our X-ray images, denoted *I*. Then, Eq. 1 is used to obtain the respiratory phase.

$$\bar{P}_{1,i} = \sum_{j \in I} P_{1,j,i} / N_I \quad (1)$$

where $P_{1,j,i}$ is the 1st dimension of HML result at patch j, frame i and N_I is the total number of patches in I. The peaks of the plots at each time frame represent end-inspiration (EI) respiratory frames, Ω_{IX}, while the troughs represent end-expiration (EX) respiratory frames, Ω_{EX}.

$$\Omega_{EI}=\left\{i|\bar{P}_{1,i-1}<\bar{P}_{1,i}>\bar{P}_{1,i+1}\right\} \tag{2}$$

$$\Omega_{EX}=\left\{i|\bar{P}_{1,i-1}>\bar{P}_{1,i}<\bar{P}_{1,i+1}\right\} \tag{3}$$

2.2 Cardiac Gating

The embedding coordinates of the 2nd dimension, P_2, of each patch for every frame of each sequence relate to the cardiac motion. However, this is significantly affected by respiratory motion. To compensate for the respiratory motion three additional steps are applied to our X-ray images, a Frangi vesselness (FV) filter [17] followed by morphological opening, morphological dilation and a band pass filter.

2.2.1 Frangi Vesselness Filter

The FV filter is applied to all X-ray images in the sequence. This technique identifies tubular structures in the X-ray images, which are expected to carry useful cardiac and respiratory motion information, using Hessian eigenvalues. The responses of the FV filter are binarised by applying a threshold. To remove the noise present while preserving the shape and size of the detected structures we apply morphological opening to the binarised responses. We denote the results of this opening process by $I_{1,i}$, where i is the X-ray frame number.

2.2.2 Morphological Dilation

The previous step is followed by the application of morphological dilation. This operation adds pixels to the boundaries of detected structures, which produces $I_{2,i}$. In morphological dilation the value of the output pixel is the maximum value of all the pixels in the input pixel's neighbourhood. Computing $I_{3,i}=I_{2,i}-I_{1,i}$ the image patches around the detected tubular structures are identified. The HML is applied to these patches only. These patches were found to be more useful for extracting cardiac motion information than using the tubular structures themselves. Although the tubular structures are expected to carry useful cardiac motion information, they also carry respiratory motion information that adversely affects the accuracy of our systolic peaks. For cardiac motion we use

$$\bar{P}_{2,i} = \sum_{j\in I_{3,i}} P_{2,j,i}/N_{I_{3,i}} \tag{4}$$

where $P_{2,j,i}$ is the 2nd dimension of the HML results at patch j, frame i and $N_{I_{3,i}}$ is the total number of patches in $I_{3,i}$.

2.2.3 Band Pass Filter and Gating

To remove residual respiratory motion, a 2nd order band pass filter is applied to our plots. The peaks of the plots represent systolic frames.

$$\Omega_{sys}=\{i|\bar{P}_{2,i\text{-}1}<\bar{P}_{2,i}>\bar{P}_{2,i+1}\} \quad (5)$$

3 Experiments

3.1 Materials

All patient procedures were carried out using a mono-plane 25cm-flat-panel cardiac X-ray system (Philips Allura Xper FD10, Philips Healthcare, Best, The Netherlands), in one of the catheterization laboratories at St. Thomas' Hospital, London, U.K. In total, 5 different clinical fluoroscopy sequences from 5 patients who underwent RFA procedures for the treatment of AF were used. A total of 284 X-ray images were processed. For each patient, X-ray imaging was performed at 3 frames per second. All X-ray images were 512×512 pixels in resolution, with a pixel to mm ratio of 0.25. Included in this ratio is the typical magnification factor of the X-ray system.

3.2 Optimization of Parameters

We built our algorithm using the leave-one-out cross-validation (LOOCV) approach. This involved using 4 sequences as the training data and the remaining sequence as the validation data. To build our algorithm, we optimised the four parameters involved in extracting the cardiac phases. These parameters include: a threshold level on the normalised output, 0 to 1, of the FV filter, the number of morphological dilations of the identified structures, and the pass band and stop band frequencies of the band pass filter, optimised to be >0.02, 30±3, 0.62 and 0.98, respectively.

3.3 Validation of Our Retrospective Cardiac and Respiratory Gating

We validated the respiratory gating using either diaphragm or heart border tracking as described in [8] for the ground truth. The choice of ground truth was determined by which structure was visible in the X-ray images. The signals obtained using the tracking method (gold standard) were compared to the signals obtained using the HML-based method. In order to validate our cardiac gating method, manual gating of the cardiac cycle at systole was performed by an experienced observer, by visually detecting the onset of contraction of the left ventricle from the fluoroscopic left heart border shadow. The systolic frame number was recorded and compared with the corresponding systolic frame number from the automatic detection. We chose systole as opposed to diastole for validation since the manual ground truth is more reliable for systole where rapid motion can be used as the visual cue.

4 Results

4.1 FV Filter and Morphological Dilation Output Images

Fig. 2(a) gives an illustration of the output of the thresholded FV filter response, $I_{1,1}$, of the first frame of one example X-ray sequence after the application of the threshold level and the morphological opening, overlaid with the corresponding X-ray image. Fig. 2(b) illustrates the image output, $I_{3,1}$, overlaid with the corresponding X-ray image for the first frame of the same example case.

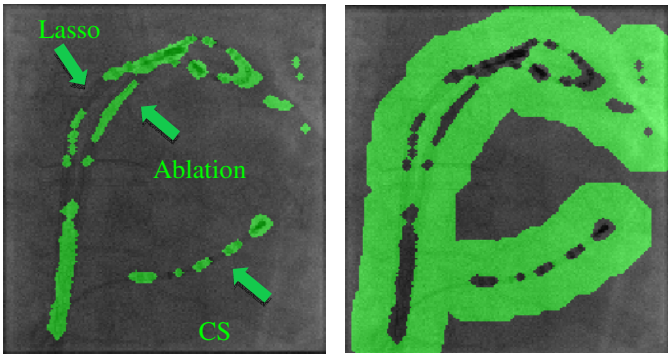

(a) (b)

Fig. 2. (a) Image output of the FV filter followed by morphological opening, $I_{1,1}$, overlaid with the corresponding X-ray image for Case 1. The EP catheters during the ablation stage of a procedure are shown. (b) Image output, $I_{3,1}$, overlaid with the corresponding X-ray image for Case 1.

4.2 Qualitative Validation

For respiratory gating validation, a plot of the respiratory trace obtained using the HML-based method for Case 1 is illustrated in Fig. 3(a) as a solid black line. The diaphragm/heart border tracking is shown as a dashed black line. The results of the cardiac gating validation are shown in Fig. 3(b) for the first 45 frames for the same case. The plotted vertical black lines correspond to the gold standard systolic frames.

4.3 Comparative Quantitative Validation

It is important to investigate whether our new HML-based technique is superior to our previously presented retrospective PCA-based gating approach [11]. Therefore, for both cardiac and respiratory gating, the absolute frame difference was computed between the HML-based method and the gold standard methods. Specifically, systolic, EI and EX frames were recorded from the HML-based and gold standard methods and their corresponding absolute frame differences were computed. This was

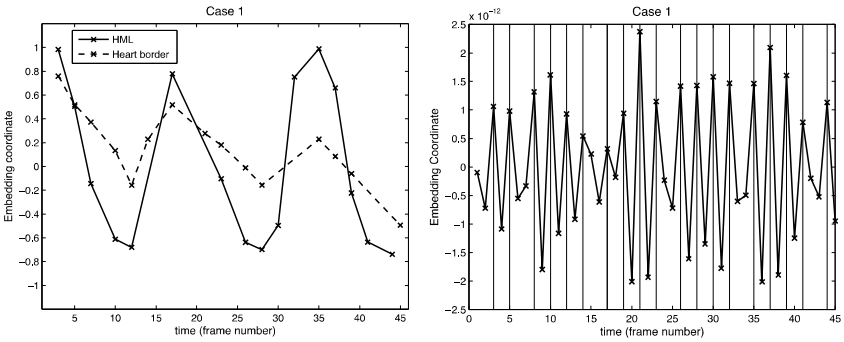

(a) (b)

Fig. 3. (a) Graphical representation of the obtained respiratory trace with X-ray frame number. The heart border tracking (gold standard) is shown as a dashed black line. (b) The HML-based method cardiac trace obtained is illustrated for the same example case. The vertical black lines are the gold standard identification of systole.

also done for the PCA-based technique. Faultless gating results are signified when the absolute frame difference between the automatic and gold standard method is zero. The results can be seen in the frequency distribution bar charts in Fig. 4(a, b and c), for EI, EX and systolic gating, respectively. Results illustrate that our HML-based method is faultless in EI and EX gating and outperforms the results of our PCA-based technique. It is also almost faultless for systolic gating. While our PCA-based technique outperforms the HML-based technique in cardiac gating, it relies on the tracking of a specific catheter, the CS catheter. Our proposed HML-based technique does not depend on any particular catheter being present in our X-ray images and requires no knowledge of catheter geometry.

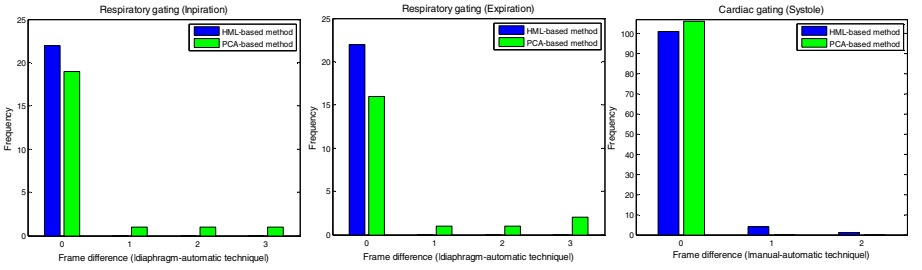

(a) (b) (c)

Fig. 4. Frequency distributions of frame difference errors for (a) End-inspiration gating (b) End-expiration gating and (c) Cardiac gating. Results are illustrated for the HML-based method (blue) and PCA-based method (green)

Percentage success rates were computed using $100\,(x/x_{total})$, where x corresponds to the number of perfectly matched gold standard and automatic gating frames and x_{total} corresponds to the total number of gold standard gating frames. Percentage success rates computed for EI, EX and systolic gating for our proposed HML-based technique were calculated to be 100%, 100% and 95.3%, respectively. For cardiac gating 4 extra false systolic peaks were obtained over all processed sequences.

5 Discussion and Conclusions

We have presented a novel and robust retrospective HML-based method for image-based automatic cardiac and respiratory motion gating. This method is able to detect cardiac and respiratory phase directly from X-ray images. We have applied our technique on 5 clinical fluoroscopy sequences and computed the success rates for EI, EX and systolic gating which were 100%, 100% and 95.3%, respectively. The HML-based method is fully automatic, requires no user interaction, no prior knowledge and can operate within a few seconds per image sequence. As our technique is not dependent on any particular catheter being present in the procedure, it has potential application in more types of cardiac catheterization procedures, rather than only RFA procedures. The method will be particularly useful for registration and overlay of pre-procedural images with X-ray fluoroscopy for guidance and biophysical modelling. Future work will focus on testing our method on X-ray coronary angiography images where no catheters are present. Investigations show that the reason for optimising systolic gating on the specified patches is because of the inclusion of the heart border, a structure that carries significant cardiac motion information. Further work will focus on modifying our technique by giving more emphasis to the importance of the heart border structure in an attempt to improve the systolic gating success rate.

Acknowledgement. This work is funded by EPSRC programme grant EP/H046410/1.

References

1. Rhode, K.S., Hill, D.L.G., Edwards, P.J., Hipwell, J., Rueckert, D., Sanchez-Ortiz, G., Hegde, S., Rahunathan, V., Razavi, R.: Registration and tracking to integrate X-ray and MR images in an XMR facility. IEEE Trans. Med. Imaging 22(11), 1369–1378 (2003)
2. Sra, J., Narayan, G., Krum, D., Malloy, A., Cooley, R., Bhatia, A., Dhala, A., Blanck, Z., Nangia, V., Akhtar, M.: Computed tomography-fluoroscopy image integration-guided catheter ablation of atrial fibrillation. Cardiovasc. Electrophysioly 18, 409–414 (2007)
3. Truong, M.V., Gordon, T., Razavi, R., Penney, G.P., Rhode, K.S.: Analysis of catheter-based registration with vessel-radius weighting of 3D CT data to 2D X-ray for cardiac catheterisation procedures in a phantom study. Statistical Atlases and Computational Models of the Heart Imaging and Modelling Challenges, 139–148 (2012)
4. Rhode, K.S., et al.: A System for Real-Time XMR Guided Cardiovascular Intervention. IEEE Trans. Med. Imaging 24(11), 1428–1440 (2005)

5. Sermesant, M., et al.: Patient-specific electromechanical models of the heart for the prediction of pacing acute effects in CRT: a preliminary clinical validation. Med. Image Anal. 16(1), 201–215 (2012)
6. Paling, M.R., Brookeman, J.R.: Respiration artifacts in MR imaging: reduction by breath holding. J. Comput. Assist. Tomogr. 10(6), 1080–1082 (1986)
7. Shechter, G., Shechter, B., Resar, J.R., Beyar, R.I.: Prospective motion correction of X-ray images for coronary interventions. IEEE Trans. Med. Imaging 24, 441–450 (2005)
8. Ma, Y.L., King, A.P., Gogin, N., Gijsbers, G., Rinaldi, C.A., Gill, J., Razavi, R.S., Rhode, K.S.: Clinical evaluation of respiratory motion compensation for anatomical roadmap guided cardiac electrophysiology procedures. IEEE Trans. Biomed. Eng. 59(1), 122–131 (2012)
9. Brost, A., Wimmer, A., Bourier, F., Koch, M., Liao, R., Kurzidim, K., Strobel, N., Hornegger, J.: Constrained registration for motion compensation in atrial fibrillation ablation procedures. IEEE Trans. Med. Imaging 31(4), 870–881 (2012)
10. Ma, Y.L., King, A.P., Gogin, N., Rinaldi, C.A., Gill, J., Razavi, R., Rhode, K.S.: Real-time respiratory motion correction for cardiac electrophysiology procedures using image-based coronary sinus catheter tracking. Med. Image Comput. Assist. Interv. 13, 391–399 (2010)
11. Panayiotou, M., King, A.P., Ma, Y.L., Rinaldi, C.A., Gill, J., Cooklin, M., O'Neill, M., Rhode, K.S.: Automatic image-based retrospective gating of interventional cardiac X-ray images. In: Conf. Proc. IEEE Eng. Med. Biol. Soc., pp. 4970–4973 (2012)
12. Sundar, H., Khamene, A., Yatziv, L., Xu, C.: Automatic image-based cardiac and respiratory cycle synchronization and gating of image sequences. In: Yang, G.-Z., Hawkes, D., Rueckert, D., Noble, A., Taylor, C. (eds.) MICCAI 2009, Part II. LNCS, vol. 5762, pp. 381–388. Springer, Heidelberg (2009)
13. Yigitsoy, C., Rijkhorst, E., Navab, N., Wachinger, C.: Manifold learning for image based breathing gating in ultrasound and MRI. Medical Image Analysis 16(4), 806–818 (2012)
14. Isguder, G.G., Unal, G., Groher, M., Navab, N., Kalkan, A.K., Degertekin, M., Hetterich, H., Rieber, J.: Manifold learning for image-based gating of intravascular ultrasound (IVUS) pullback sequences. In: Liao, H., "Eddie" Edwards, P.J., Pan, X., Fan, Y., Yang, G.-Z., et al. (eds.) MIAR 2010. LNCS, vol. 6326, pp. 139–148. Springer, Heidelberg (2010)
15. Bhatia, K.K., Rao, A., Price, A.N., Wolz, R., Hajnal, J., Rueckert, D.: Hierarchical manifold learning. In: Ayache, N., Delingette, H., Golland, P., Mori, K. (eds.) MICCAI 2012, Part I. LNCS, vol. 7510, pp. 512–519. Springer, Heidelberg (2012)
16. Belkin, M., Niyogi, P.: Laplacianeigenmaps for dimensionality reduction and data representation. Neural Computation 15(6), 1373–1396 (2003)
17. Frangi, A.F., Niessen, W.J., Vincken, K.L., Viergever, M.A.: Multiscale vessel enhancement filtering. In: Wells, W.M., Colchester, A.C.F., Delp, S.L. (eds.) MICCAI 1998. LNCS, vol. 1496, pp. 130–137. Springer, Heidelberg (1998)